arXiv:1006.0171v1 [physics.ins-det] 14 May 2010

# Advances in Modeling of Scanning Charged-Particle-Microscopy Images

Petr Cizmar, András E. Vladár, and Michael T. Postek

National Institute of Standards and Technology (NIST) *, 100 Bureau Drive, Gaithersburg, MD 20899, USA

## ABSTRACT

Modeling artificial scanning electron microscope (SEM) and scanning ion microscope images has recently become important. This is because of the need to provide repeatable images with a priori determined parameters. Modeled artificial images are highly useful in the evaluation of new imaging and metrological techniques, like image-sharpness calculation, or drift-corrected image composition (DCIC). Originally, the NIST-developed artificial image generator was designed only to produce the SEM images of gold-on-carbon resolution sample for image-sharpness evaluation. Since then, the new improved version of the software was written in C++ programming language and is in the Public Domain. The current version of the software can generate arbitrary samples, any drift function, and many other features. This work describes scanning in charged-particle microscopes, which is applied both in the artificial image generator and the DCIC technique. As an example, the performance of the DCIC technique is demonstrated.

## 1. INTRODUCTION

Computational scanning electron microscopy[1] through rapid artificial image modeling is gaining importance. It is a useful tool for evaluation of imaging and metrology methods, since real SEMs or other charged-particle microscopes cannot always provide repeatable images. For example, it is virtually impossible to obtain two real SEM images that only differ in random noise. This is usually caused by many perturbing factors like drift, sample charging, or electro-magnetic fields. The artificial image generator is capable of modeling all important effects in a deterministic way. One can a priori choose the drift function, the type[2,3] and magnitude and type of noise, the charged-particle-beam profile, etc. That being the case, computer generated artificial images may be input to the imaging and metrological techniques and the results compared to the chosen parameters, hence indicating the performance of given techniques. None of these is possible with the real images, where these effects are present there, but all are random and often even unknown.

An advanced version of the artificial SEM image generator[4,5] has been released as a public-domain software. It is implemented as a library written in C++. This also allows for linking with programs written in many other programming languages. The software works in Linux, Mac OSX, Windows, and very probably in other UN*X systems as well, however, the latter has not yet been tested. For faster and easier designing of calculations, Lua[6] scripting was implemented. Lua is a scripting language originally designed for data-entry applications. These days it is mostly employed in computer games. It is one of the simplest and fastest scripting languages available. A simple graphical user interface (GUI) has been written mainly for demonstration. One can very easily generate images of two types; gold-on-carbon resolution sample and periodic semiconductor cross structures. The GUI depends on wxWidgets[7] library which is multiplatform as well.

One of the techniques that have been tested with modeled images is the drift-corrected image composition (DCIC),[8] which outputs significantly more accurate images than the traditional imaging techniques. This is necessary for sub-nanometer-scale metrology, since the conventional "slow-scan" and "fast-scan" techniques provide images that are often distorted or blurry. The DCIC works with frames that are taken as quickly as the capabilities of the instrument permit. Physical drift causes displacement between each couple of frames. This displacement is searched for with cross-correlation. Since the quickly acquired frames are usually extensively noisy, a noise reduction is a part of the DCIC technique.

* Contribution of the National Institute of Standards and Technology; not subject to copyright. Certain commercial equipment is identified in this report to adequately describe the experimental procedure. Such identification does not imply recommendation or endorsement by the National Institute of Standards and Technology, nor does it imply that the equipment identified is necessarily the best available for the purpose.

## 2. DRIFT DISTORTION

In the scanning microscopes, the image is formed by scanning across the sample in a raster pattern. Intensity value is acquired at each location on the sample. In digital scanning microscopes, that corresponds with a pixel in the image. The intensity value $\xi(\vec{r})$ depends on the landing position of the electron beam $\vec{r}$. Most SEMs use the raster pattern. Let the raster pattern be defined by the time-dependent vector function:

$$\begin{aligned}
\vec{r}_r(t) &= M\left(x(t)\vec{e}_x + y(t)\vec{e}_y\right), &(1)\\
t_p &= t_D + t_d, &\\
y(t) &= \left\lfloor \frac{t}{Xt_p + t_j} \right\rfloor, &(2)\\
x(t) &= \left\lfloor \frac{t}{t_p} \right\rfloor - Xy(t), &(3)\\
0 \leq \; t &\leq Y(Xt_p + t_j), &
\end{aligned}$$

where $t$ is time, $M$ is a single-pixel step length. $x$ and $y$ are column and row indexes in the SEM image. $\vec{e_x}$ and $\vec{e_y}$ are the unit vectors in x- and y-direction, $t_D$ is the pixel-dwell time, $t_d$ is the dead time between acquisition of two pixels, $t_j$ is the time needed to move the beam to the beginning of the new line. $\lfloor q \rfloor$ is a symbol for the floor($q$) function as used in programming languages. $X$ and $Y$ are the pixel-width and pixel-height of the SEM image.

Let the SEM imaging be defined as a relation between the intensity map of the sample $\xi(\vec{r})$ and the SEM image $I(x, y)$:

$$I(x(t), y(t)) = K\xi(\vec{r}(t)). \tag{4}$$

The relation between $I$ and $\xi$ may in practice be very general. For simplicity, let $K$ be a constant in this manuscript, since this does not affect generality of the DCIC technique. In the ideal case: $\vec{r}(t) = \vec{r}_r(t)$; however, drift and space distortions are always present in scanning microscopes and they can significantly affect the position $\vec{r}$:

$$\vec{r}(t) = \vec{r}_r(t) + \vec{D}_d(t) + \vec{D}_s(\vec{r}_r). \tag{5}$$

The space distortion $\vec{D}_s$ is constant in time and may be compensated for, when its function is known. This distortion may be caused by non-linearities in deflection amplifiers and is significant mostly at low magnifications. On the other hand, the drift distortion $\vec{D}_d$ is changing in time, its function is usually unknown, and it may extensively affect the high-magnification images. The drift distortion may arise from several sources; e.g. translational motion of the sample, tilt or deformation of the electron-optical column, outer forces and vibrations, or temperature expansion. High-magnification images are very sensitive to drift distortion, since microscopic displacements, tilts, or temperature changes can easily cause nanometer distortions and displacements, which can significantly impair the SEM image and its usability for nanometer-scale measurements.

The drift-distortion function is generally unknown, however, since it characterizes motion of physical bodies, it must be continuous and thus square-integrable. Therefore, drift-distortion function may be Fourier-series expanded:

$$\begin{aligned}
D_{cd}(t) &= \sum_{n=-\infty}^{\infty} c_n \mathrm{e}^{-int}, &(6)\\
\vec{D}_d &= \Re(D_{cd})\vec{e}_x + \Im(D_{cd})\vec{e}_y, &(7)\\
U &\propto \sum_{n=-\infty}^{\infty} c_n^2 n^2, &(8)
\end{aligned}$$

where $c_n$ are the (complex) Fourier coefficients, $U$ is the overall energy of the drifting system. Since $U$ is limited, for high $n$ the coefficients $c_n$ must be nearing zero. In practice, for frequencies higher than 200 Hz, $c_n$ correspond

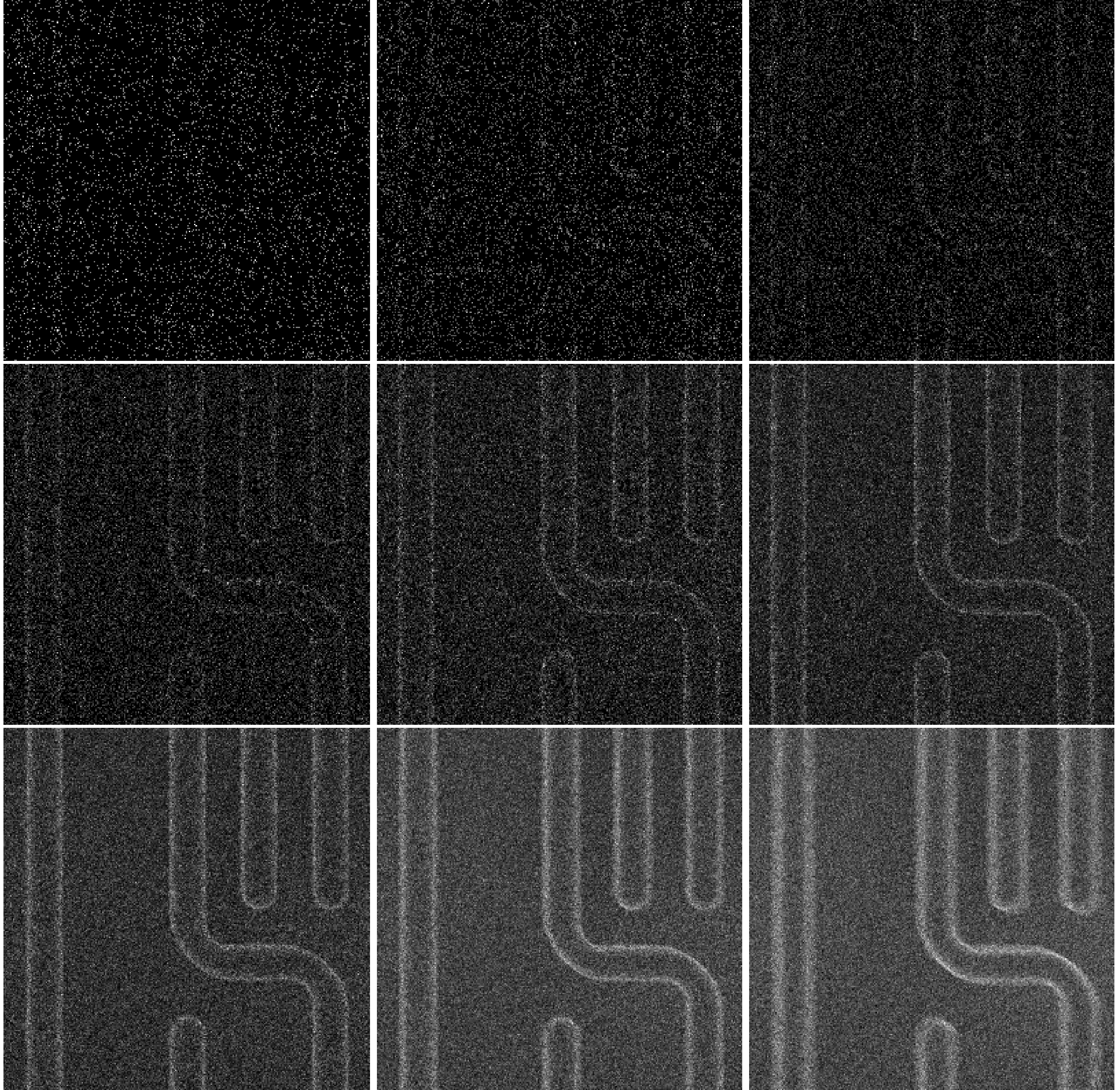

Figure 1. Series of artificial images of a semiconductor structure composed using the traditional "fast-scan" technique. Compositions of 2, 4, 8, 16, 32, 64, 128, 256, and 512 frames (from the top left). Images are normalized.

to noise only and are negligible. Therefore, the $D_{cd}(t)$ can be written:

$$D_{cd}(t) \approx \sum_{n=-N}^{N} c_n \mathrm{e}^{-\mathrm{i}nt}, \tag{9}$$

where $N$ represents the highest significant angular frequency.

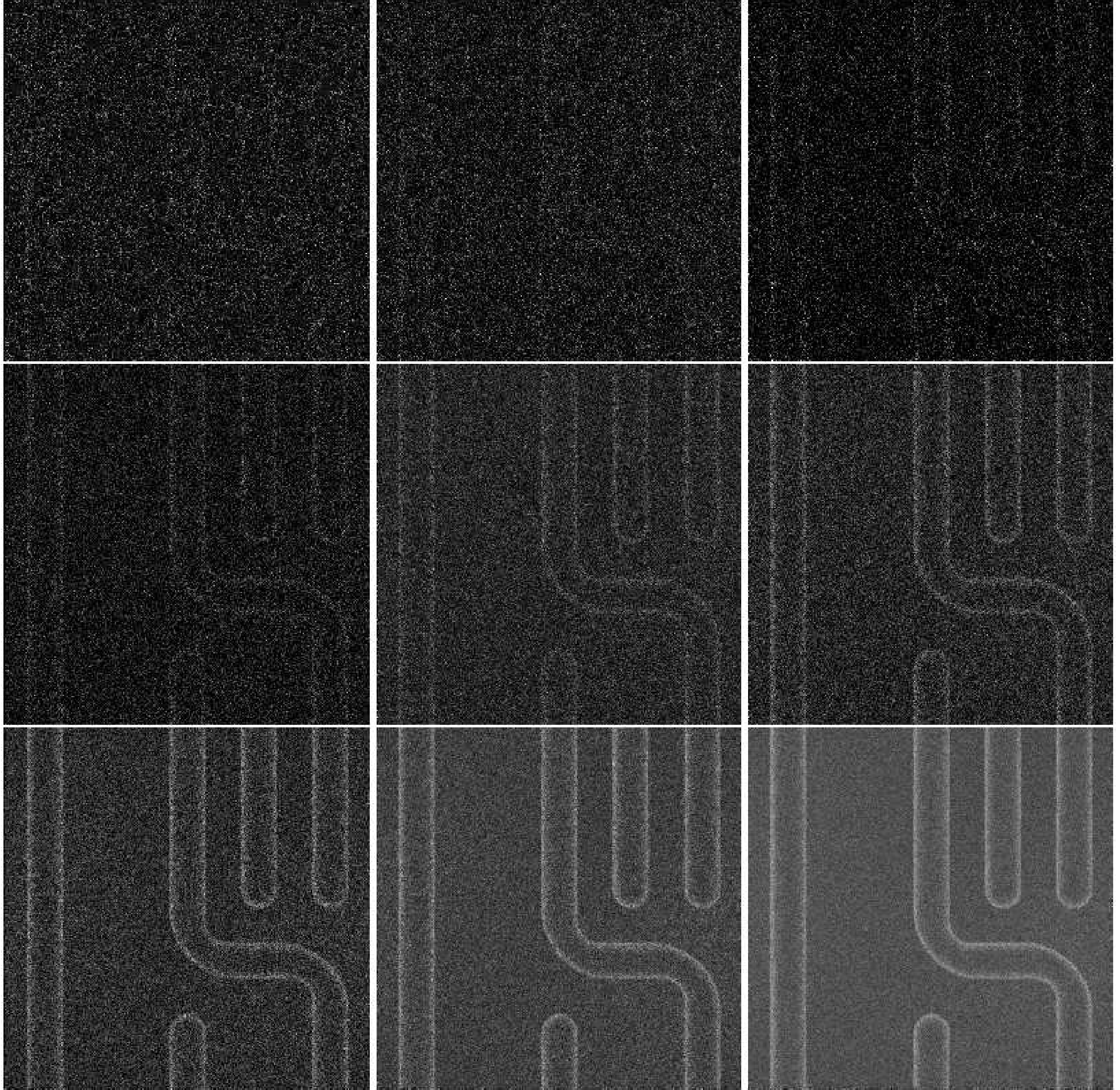

Figure 2. Series of artificial images of a semiconductor structure composed using the DCIC method. Compositions of 2, 4, 8, 16, 32, 64, 128, 256, and 512 frames (from the top left).

## 3. "FAST-SCAN" IMAGING

The imaged intensity signal in the SEM always contains noise. The intensity function is a superposition of a real signal and noise:

$$\xi(\vec{r},t) = \xi_s(\vec{r}) + \xi_n(t), \tag{10}$$

where $\xi_s$ is the position-dependent real signal and $\xi_n$ is the time-dependent noise. $\xi_n$ is a superposition of all noise contributions present in the SEM: Poisson noise originating from the electron source and the secondary emission, the noise originating from the amplifier and electronics, quantization-error noise, etc. Due to the central limit

theorem, it is legitimate to suppose that the mean value of this noise is zero:

$$< \xi_n(t) >= 0. \tag{11}$$

In order to obtain a SEM image with a desired level of noise, the overall pixel dwell-time $t_D$ must be sufficiently high. Unfortunately, the electron yield is usually low and the overall pixel-dwell time must often be set to times ranging from tens to several hundreds of $\mu$s.

In the SEM, there are two common methods to achieve this, i.e "slow-scan" and "fast scan", while the latter is useful for metrological application.

"Fast-scan" is one of the common imaging methods in SEMs. The image is composed from multiple ($N$) frames, for which averaging is the mostly applied technique. The frames are acquired with the lowest possible pixel-dwell time $t_D$. The image pixel value is an average of corresponding frame-pixel values:

$$\begin{aligned} I_k(x(t_0), y(t_0)) &= K\xi_s(\vec{r}(t_0 + kt_f)) + \\ &+ K\xi_n(t_0 + kt_f), \qquad (12) \\ I(x,y) &= \frac{1}{N}\sum_{k=0}^{N} I_k(x,y). \qquad (13) \\ t_f &= Y(Xt_p + t_j) + t_{jj}, \qquad (14) \end{aligned}$$

$t_f$ is a time period between beginnings of acquisition of two following frames, $t_{jj}$ is the dead time between the end of acquisition of one frame and beginning of the next one. Considering Eq (11), the higher $N$, the lower noise level is present in the image. The required noise-level thus determines the number of composed images $N$. For high $N$:

$$\sum_{k=0}^{N-1} \xi_n(t_0 + kt_f) \approx 0. \tag{15}$$

Because the scanning raster pattern is constant for all frames,

$$\vec{r}_r(t_0 + kt_f) = \vec{r}(t_0). \tag{16}$$

Eq (12) may be expanded:

$$\begin{aligned} I(x(t_0), y(t_0)) &= \frac{K}{N}\sum_{k=0}^{N-1} \xi_s[\vec{r}_r(t_0) + \\ &+ \vec{D}_s(\vec{r}_r(t_0)) + \vec{D}_d(t_0 + kt_f)]. \qquad (17) \end{aligned}$$

With current SEMs, the frame-acquisition time $t_f$ can be much lower than the period of even the highest drift-distortion frequencies. The drift-distortion within the single-frame acquisition time is then minimal. However, it becomes significant during acquisition of the whole image, especially, when the dead times $t_{jj}$ are prohibitively high, which is the case even with some current instruments.

## 4. DRIFT-CORRECTED IMAGE COMPOSITION (DCIC)

The "fast-scan" method may be significantly improved using drift-distortion correction, when the images are acquired quickly enough. Since the space-distortion $\vec{D}_s$ is much less pronounced and much smaller that the drift-distortion $\vec{D}_d$ at very high magnifications, it will be neglected from now on. The Eq (17) then becomes:

$$\begin{aligned} I(x,y) &= \frac{K}{N}\sum_{k=0}^{N-1} \xi_s[\vec{r}_r(r) + \vec{D}_{dk}], \qquad (18) \\ \vec{D}_{dk} &= \vec{D}_d(t_0 + kt_f). \qquad (19) \end{aligned}$$

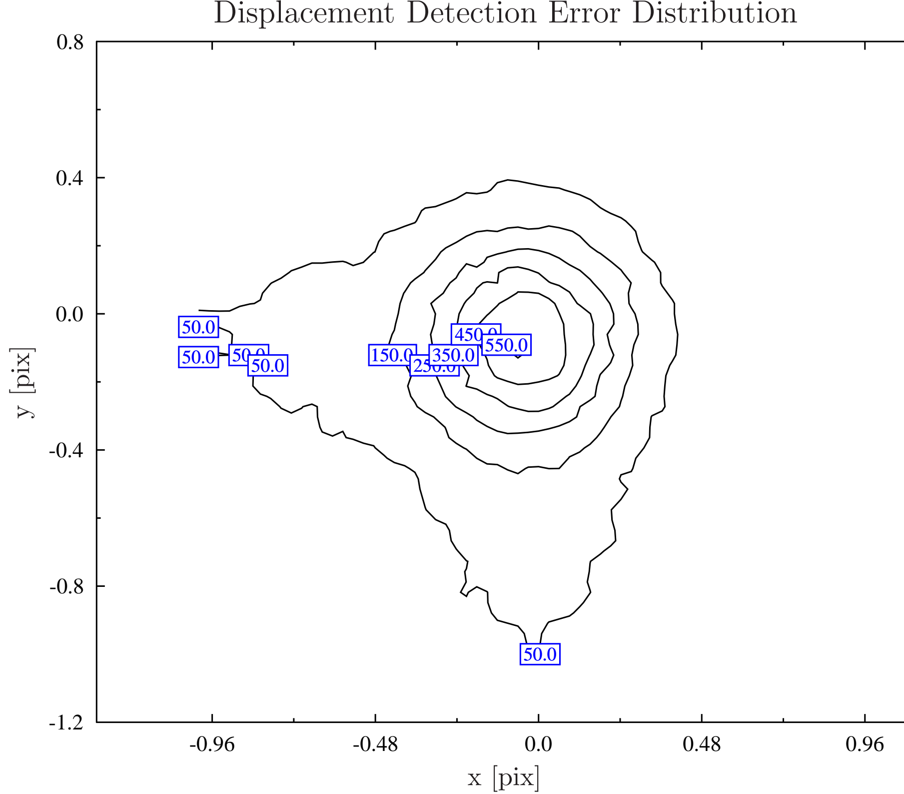


Figure 3. Error distribution of the displacement detection. Artificial SEM image of a periodic semiconductor sample was used.

The image is in this case the mean value of $N$ displaced images.

Under certain conditions, it is possible to find the displacement vectors of the images, which are equal to the drift-distortion values $\vec{D}_{dk}$. The drift-distortion then may be compensated for, which allows for acquisition of a corrected, more accurate image. One possible approach is a cross-correlation-based displacement detection, which is used in the DCIC technique. The maximum of the cross-correlation function is searched for. Its position is equal to the searched displacement vector $\vec{D}_{dk}$.

In the DCIC technique, the cross-correlation with noise reduction is applied. This is necessary, because the quickest-acquired images are usually very noisy and the peak in the cross-correlation function becomes overridden by numerous other peaks, corresponding to random correlation of noise. This often makes finding the displacement vector impossible. This issue can be tackled by low-pass frequency filtering performed in the frequency domain. The cut-off frequency is determined by the filter-radius $R$.

Plain maximum search in a discrete function limits the accuracy to a minimum of one pixel. However, in the DCIC, the detection of the displacement vector $\vec{D}_{dk}$ is performed with sub-pixel resolution. The peak in the two-dimensional cross-correlation function is interpolated with a polynomial third-order two-dimensional polynomial function and the algorithm then searches for its maximum.

The technique is very powerful, since it can correct for the drift-related distortions and blur in extremely noisy images. (See Figs 1 and 2)

## 5. ACCURACY OF THE DCIC TECHNIQUE

The accuracy of the detected displacement vector $\vec{D}_{dk}$ characterizes the accuracy of the DCIC imaging technique. Errors in the displacement vector can cause blur. Such blur can under certain circumstances be larger than with

application of the original "fast-scan" technique ($\vec{D}_{dk} = \vec{0}$). In metrological applications, where dimensions are measured from the images, the drift-related displacement is the main source of errors.

The artificial SEM images have been successfuly used to evaluate accuracy of the DCIC technique. The artificial-image generator is, unlike any other source of SEM images, capable of modeling all necessary characteristics for this application, e.g. arbitrary drift functions, dead times, arbitrary types of samples, etc.

A performance characteristics must be chosen to investigate the limits of an imaging technique. Application of the standard deviation of the displacement vector would be a good candidate, if the distribution of errors was Gaussian. In order to find this out, a large set of artificial images (500 000) randomly differing in displacement and noise has been applied to find the error distribution of the displacement detection. The DCIC technique has processed all generated frames and has output corresponding displacement values. The two-dimensional histogram of these values forms the resulting distribution, which is shown in the Fig 3. These data have clearly indicated that the error distribution is not (always) Gaussian. Using standard (Gaussian) error processing has therefore been unsuitable and thus we have chosen the mean error $\delta_D$ as the performance characteristics.

$$\bar{\delta}_D = \frac{1}{N-1} \sum_{k=1}^{N-1} \delta_{Dk}, \tag{20}$$

where $\delta_{Dk}$ is the error of the displacement vector $\vec{D}_{dk}$ and $N$ is the number of frames. Since the correct displacement vector $\vec{D}_{ci}$ is known (it is determined by the artificial-image generator),

$$\delta_{Dk} = |\vec{D}_{dk} - \vec{D}_{ck}|. \tag{21}$$

The performance of the DCIC technique is obviously limited, because noise, blur, contrast, and other parameters affect it significantly. For instance, if the frames were extremely blurred and the cross-correlation maximum would be overly wide and the mean error of the displacement vector would be excessively high. It is therefore useful to find the dependences of $\delta_D$ on noise and blur and provide a set of limiting parameters.

The dependence of the mean error of the detected displacement $\bar{\delta}_D$ on noise and blur have been both investigated with application of artificial images. Gaussian noise and Gaussian blur have been chosen for simplicity, although the type of noise and the blur profile may be arbitrary. For every step in noise and blur, 5000 artificial images of the gold-on-carbon resolution sample have been generated and processed by the DCIC algorithm. The results of these tests are shown in Figs 4 and 6. For reference images showing different magnitudes of Gaussian noise see Fig 5. These tests demonstrate the capability of the DCIC technique to find the displacements with sub-pixel accuracy. In the noise test, this is maintained up to the $\sigma_g = 8$, which roughly corresponds to signal to noise ratio (SNR) around 0.1 and the dependence is almost linear. The dependence on blur indicates that the sub-pixel accuracy is sustained up to $\sigma_b = 14$.

## 6. CONCLUSION

Modeled artificial SEM images were first employed in assessment of the image-sharpness calculation techniques[1] and have been adopted as a part of the developed international standard for image sharpness. Since then, a new highly improved version of the software was written. This version supports arbitrary non-overlapping two-dimensional samples, rigorous generation of Poisson and Gaussian noise, arbitrary drift functions, dead times and other features. Scripting in Lua scripting language was implemented to make the calculations easier to design. This new tool was then used in evaluation of the new imaging technique of DCIC. By finding dependence of the error in detection of the displacement on noise and blur, the sub-pixel accuracy was demonstrated even for high magnitudes of noise or blur. This makes the DCIC and modeling of microscope images useful and important tools for nanoscale metrology and nanotechnology.

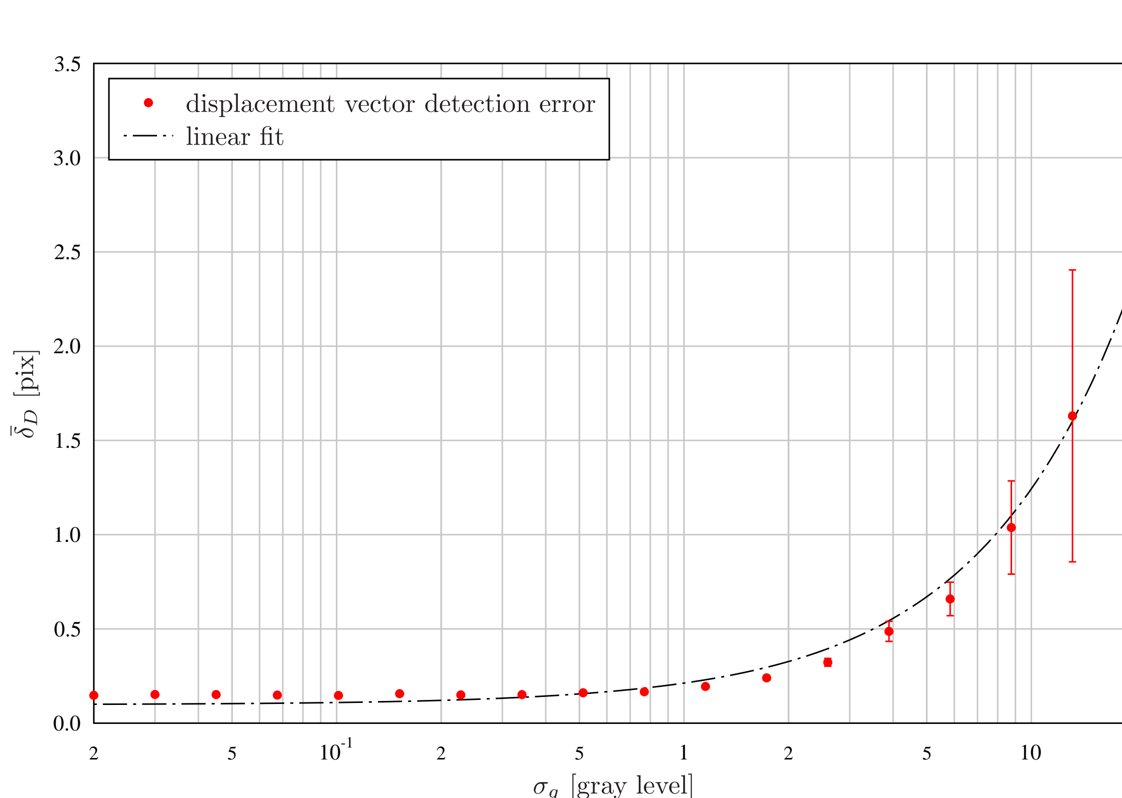


Figure 4. Evaluation of the DCIC technique. Dependence of the mean displacement detection error on the magnitude ($\sigma_g$) of Gaussian noise. Each represents 5000 artificial images of the gold-on-carbon resolution sample sized 512x512 pixels. The error-bars denote the standard deviation of the displacement vector detection error.

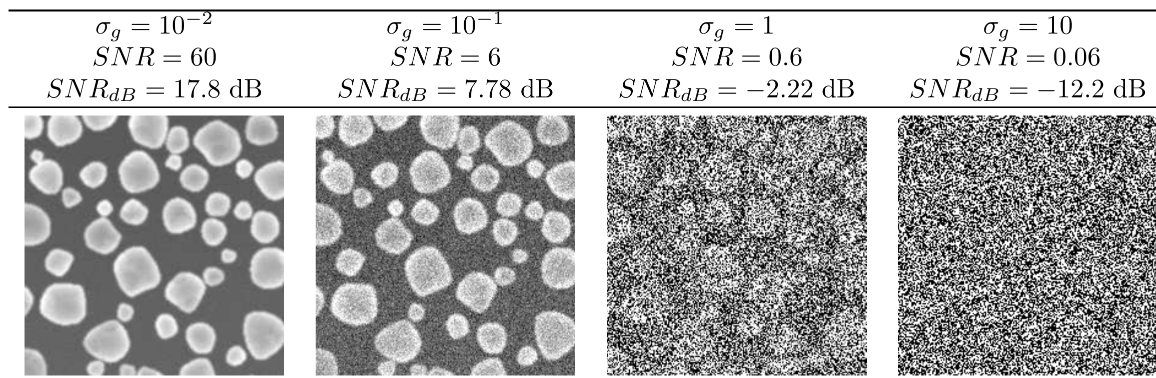


Figure 5. Gaussian-noise scale. Artificial images of the gold-on-carbon resolution sample with Gaussian noise of different magnitudes.

## REFERENCES

1. M. T. Postek, A. E. Vladar, J. R. Lowney, and W. J. Keery, "Two-dimensional simulation and modeling in scanning electron microscope imaging and metrology research," *Scanning* **24**, pp. 179–185, JUL-AUG 2002.
2. G. E. P. Box and M. E. Muller, "A Note on the Generation of Random Normal Deviates," *Annals of Mathematical Statistics* **29**(2), pp. 610–611, 1958.
3. D. E. Knuth, *Art of Computer Programming, Volume 2: Seminumerical Algorithms*, Addison-Wesley Professional, third ed., November 1997.

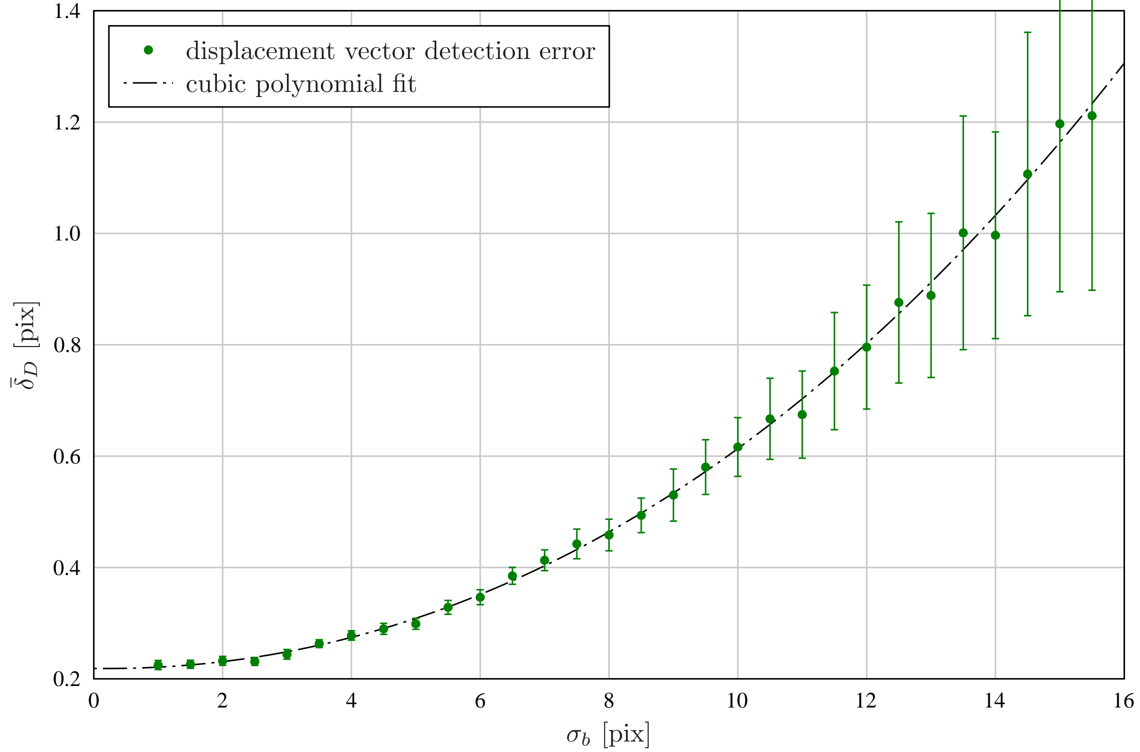


Figure 6. Evaluation of the DCIC technique. Dependence of the mean displacement detection error on Gaussian blur ($\sigma_b$). This blur simulates the effect of the charged-particle-beam profile. Each represents 5000 artificial images of the gold-on-carbon resolution sample sized 512x512 pixels. The error-bars denote the standard deviation of the displacement vector detection error.

4. P. Cizmar, A. E. Vladar, B. Ming, and M. T. Postek, "Simulated SEM Images for Resolution Measurement," *Scanning* **30**, pp. 381–391, Sep-Oct 2008.
5. P. Cizmar, A. E. Vladar, and M. T. Postek, "Optimization of accurate sem imaging by use of artificial images," *Scanning Microscopy 2009* **7378**(1), p. 737815, SPIE, 2009.
6. R. Ierusalimschy, L. H. de Figueiredo, and W. Celes, *Lua 5.1 Reference Manual*, Lua.org, 2006.
7. J. Smart, K. Hock, and S. Csomor, *Cross-Platform GUI Programming with wxWidgets*, Prentice Hall, 2005.
8. P. Cizmar, A. E. Vladar, and M. T. Postek, "Real-Time Image Composition with Correction of Drift Distortion," *ArXiv e-prints* , Oct. 2009.